Microchimica Acta (2021) 188:253
https://doi.org/10.1007/s00604-021-04917-8

ORIGINAL PAPER

Fluorescent detection of microRNA-21 in MCF-7 cells based on multifunctional gold nanorods and the integration of chemotherapy and phototherapy

Yan Gong[1] · Wei Yuan[1] · Xinjie Guo[1] · Qian Zhang[1] · Peng Zhang[1] · Caifeng Ding[1]

Received: 15 March 2021 / Accepted: 26 June 2021

Abstract

MicroRNA-21 is an important biomarker of tumor early prediction and metastasis, and its accurate detection is of great significance for tumor diagnosis and treatment. It will be a meaningful work to combine the detection of RNA with chemotherapy and photothermal therapy on the same composite material. Herein, we designed a multifunctional nanocomposite based on gold nanorods (AuNRs), making use of microRNA-triggered drug release and near-infrared photothermal effect, which has been developed for cancer therapy and microRNA-21detection. Firstly, the AuNRs with photothermal effect were synthesized as carriers for drug delivery. Then the surface of gold nanorods was modified by functional DNA chains to provide an efficient site for doxorubicin (DOX) loading. Finally, folic acid was introduced to achieve the targeted treatment of MCF-7 cells. The microRNA competed with the double-stranded DNA, resulting in the release of DOX and the recovery of fluorescence signal located at 595 nm with an excitation of 488 nm effectively. The nano-biosensor could not only achieve dual-function of diagnosis and treatment of cancer cells, but also accomplish the detection of microRNA in tumor cells. It showed a high selectivity for microRNA-21 determination with a limit of detection (LOD) of 2.1 nM from the linear relationship from 1.0×10^{-5} M to 5.0×10^{-7} M. This scheme provides an outstanding strategy for cell imaging, treatment, and detection, which serves as a promising candidate in the field of biomedical research.

Keywords Fluorescent nanoprobe · microRNA-21 · Chemo-photoacoustic therapy · Drug delivery · Cell imaging

Introduction

MicroRNA, a short non-coding sequence, is usually composed of 19–25 nucleotides [1, 2]. It can regulate genetic diversity by inhibiting gene translation or improving microRNA degradation. MicroRNA plays an important role in the early division of living cells and virus [3]. In addition, some related reports showed that the overexpression of microRNA-21 is closely related to the drug resistance of tumor cells [4, 5]. Therefore, microRNA-21 has become a biomarker for tumor early prediction and metastasis and is a potential "seed carrier." For example, breast cancer, cervical cancer, lung cancer, and pancreatic cancer are related to overexpression of microRNA-21 [6].

At present, the traditional detection methods for microRNA include quantitative fluorescence reverse transcription PCR (RT-PCR) [7–9], northern blotting [10, 11], and microarray [12–14]. RT-PCR has the advantages of high sensitivity and specificity, but it needs reverse transcription for the cDNA before amplification, which makes it difficult to conduct highly parallel qRT-PCR according to sequence specificity during primer annealing. Northern blotting can be used for semiquantitative detection and analysis of microRNA, but the sensitivity is limited. Microarray technology can detect multiple microRNA samples in a short time, but it has poor repeatability and low sensitivity. In recent years, many methods have been developed to detect microRNAs, such as Raman spectroscopy, mass

✉ Qian Zhang
zhangq_chem@qust.edu.cn

✉ Caifeng Ding
dingcaifeng@qust.edu.cn

[1] Key Laboratory of Optic-electric Sensing and Analytical Chemistry for Life Science, MOE, Shandong Key Laboratory of Biochemical Analysis, Key Laboratory of Analytical Chemistry for Life Science in Universities of Shandong, College of Chemistry and Molecular Engineering, Qingdao University of Science and Technology, Qingdao 266042, China

Published online: 14 July 2021

spectrometry, and electrochemiluminescence. Although these methods have high sensitivity, they can hardly meet the requirements of microRNAs detection in living cells. Moreover, due to the low expression of microRNA in living cells and the urgent need for early diagnosis and treatment, it is important to provide a rapid and sensitive method to detect microRNA in living cells.

Doxorubicin (DOX) is a kind of widespread anti-tumor drug, and its mechanism of action is mainly to inhibit cell growth through DNA interference and the formation of free radicals [15]. Although DOX is widely used in clinic, there are still many problems, such as non-specific drug delivery, short half-life, drug resistance caused by long-term drug treatment, and other side effects [16]. In order to solve these issues, we need to improve the drug delivery method to achieve targeted and sustained release of DOX. It is an effective method to develop nanoparticles with multifunctional targeted drug delivery [17].

In recent years, AuNRs have attracted much attention because of the unique optical and chemical properties. Various molecules, such as antibodies, peptides, nucleic acids, and carbohydrates, can be modified on the surface of AuNRs by ligand exchange, so as to further enhance biocompatibility and the ability of targeted drug delivery [18, 19]. In addition, AuNRs show strong absorption in the near-infrared (NIR) and visible region. The excitation light of surface plasmon resonance (SPR) can be used as a photothermal contrast agent for cancer diagnosis and imaging [20]. In general, it is difficult for drugs to directly enter the tumor tissue through the blood circulation. To increase the volume of blood flow around the tumor tissue and vascular permeability by means of photothermal therapy [21–28], the ability of target drug delivery needs further enhancement. AuNRs will produce strong photothermal effects after absorbing photons. Therefore, photothermal therapy and chemotherapy can be combined to improve the delivery and accumulation of drugs in tumor cells.

In this work, AuNRs were used as a model of nano-carrier for drugs and photothermal agent to induce cell apoptosis, and a functional gold nanoprobe for in situ microRNA-21 imaging and cell diagnosis was designed. As shown in Scheme 1, the molecular beacons (MBs) that the ends of two hybrid DNA strands were in a state of base mismatch were connected with AuNRs to build functional fluorescence probes. Folic acid (FA) was modified on the surface of AuNRs as a signal molecule to specifically recognize breast cancer cells (MCF-7), and then DOX was inserted into the grooves of double-stranded DNA to successfully prepare AuNRs-DNA/FA: DOX nanoprobe. The fluorescence signal of DOX was effectively quenched by AuNRs due to fluorescence resonance energy transfer (FRET). Because the receptor protein on the membrane surface of MCF-7 cell can specifically recognize FA, the nanoprobe entered the cancer cells through endocytosis after the AuNRs-DNA/FA: DOX probe was incubated with MCF-7 cells. MicroRNA-21 was overexpressed in MCF-7 cells, and one of the DNA strands was complementary to microRNA-21, so microRNA-21 will compete with the double-stranded DNA of the nanoprobe, leading to the open of double-stranded MB, the release of DOX from the double-stranded DNA, and the recovery of fluorescence signal. The photothermal effect of AuNRs under the irradiation of NIR light, along with DOX chemotherapeutic performance, endows the nanocomposite with both photothermotherapy and chemotherapy, which can promote cell apoptosis and provide an effective way for real-time monitoring of microRNA-21 content and treatment of tumor.

Experimental section

Preparation of AuNRs-DNA/FA

Firstly, 2 mg EDC was added into 500 μL of 9 mM FA and stirred for 20 min, and then 0.1 mg NHS was added into the mixture, and the mixture reacted for 1 h. The activated FA was reacted with SH-PEG-NH_2 for 12 h, and the product was filtered by dialysis (MWCO = 1000) for 24 h to obtain the pure SH-PEG-FA. Finally, 10 μL SH-PEG-FA was reacted with AuNRs-DNA for 12 h, and the pure AuNRs-DNA/FA solution was obtained by centrifugation (10 min, 9000 rpm).

Preparation of AuNRs-DNA/FA: DOX

Ten microliters of 1 μM DOX was reacted with AuNRs-DNA/FA at room temperature for 12 h, and the pure nanocomposite probe (AuNRs-DNA/FA: DOX) was obtained by centrifugation (10 min, 9000 rpm) and washing.

AuNRs-DNA/FA: DOX for microRNA-21 detection

Ten microliters of AuNRs-DNA/FA: DOX nanoprobe was incubated with different concentrations of microRNA-21 (8.0×10^{-5}, 5.0×10^{-5}, 2.5×10^{-5}, 1.0×10^{-5}, 8.0×10^{-6}, 5.0×10^{-6}, 2.5×10^{-6}, 1.0×10^{-6}, 5.0×10^{-7}, 1.0×10^{-7}, 5.0×10^{-8}, 1×10^{-8}, 5×10^{-9}, 1.0×10^{-9} M) at room temperature for 2 h, and the fluorescence intensity of the supernatant was measured (λ_{ex} = 488 nm, λ_{em} = 595 nm).

Culture of MCF-7 and HeLa cells

Firstly, the environment of culture was sterilized with ultraviolet lamp, then the culture medium of MCF-7 cells and HeLa cells was poured out, and 0.5 mL trypsin was added to the two bottles respectively to harvest the cells. After incubating for 2 min, it was observed that the shape of the cells became round and shiny under microscope, and then 2 mL of the culture

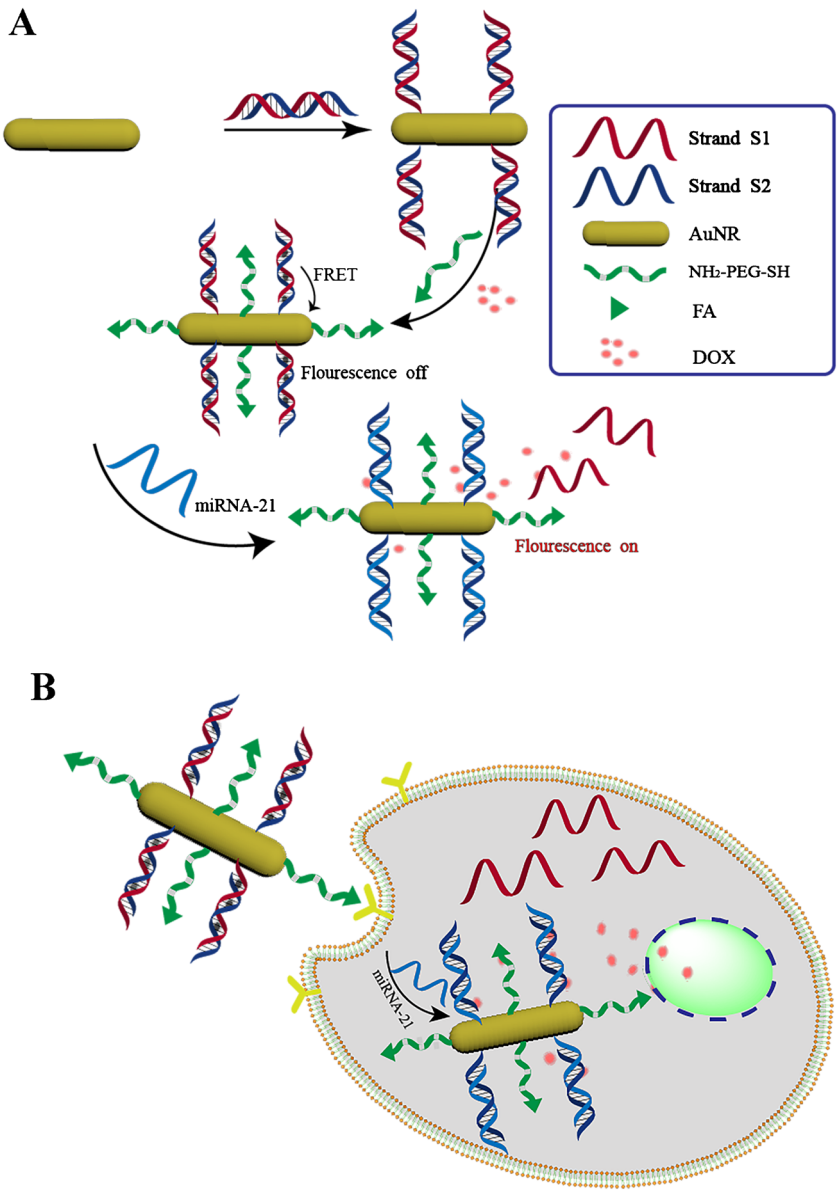

Scheme 1 **A** Schematic illustration of synthesis of AuNRs-DNA/FA: DOX and its response to microRNA-21. **B** Detection and treatment mechanism of AuNRs-DNA/FA: DOX in cell

media was added to the two bottles to quench the reaction. Finally, the cells were dispersed in petri dishes for culture.

Cytotoxicity evaluation by CCK-8

The 96-well plate was disinfected with UV light, and then 10 μL PBS was added to the outermost hole of the plate to prevent liquid volatilization. After that, 100 μL of harvested MCF-7 cells were added to the inner layer and cultured in the incubator for 48 h. After the bottle wall was covered by the cells, the culture medium in the inner layer of the plate was changed, and 5 μL AuNRs-DNA/FA nanocomposites were added into three holes respectively and incubated. After that, AuNRs-DNA/FA nanocomposites were added to the three holes every 1 h, 2 h, 4 h, 8 h, 12 h, 24 h, and 48 h, respectively. Finally, 10 μL CCK-8 stain was added into each well, and the cell survival rate was measured by enzyme labeling instrument after incubating for another 5 h.

Confocal fluorescence imaging after NIR irradiation

MCF-7 cells and HeLa cells were seeded into petri dishes and incubated in CO_2 incubator for 48 h. The prepared 5 μL nanoprobe was added to the petri dish and incubated for 2 h. After being irradiated for 5 min with 808 nm pulse laser (1000 mW), the fluorescence signals of the cells were observed from 570 to 630 nm by confocal laser scanning microscope with the excitation wavelength of 488 nm.

Transfection of HeLa cells

The expression of microRNA-21 in HeLa cells was regulated by cell transfection. First, 190 μL and 200 μL DMEM were added into two centrifuge tubes after treated with DEPC labeled A and B. Twelve microliters of RNATrans Mate was added into tube A, and 2 μL microRNA-21 mimic (or microRNA-21 inhibitor) (20 μM) was added into tube B, respectively. Then tube A and B were mixed and incubated at room temperature for 10 min to form a microRNA-21 mimic (or microRNA-21 inhibitor)/RNATrans Mate complex. After that, 100 μL microRNA-21 mimic (or microRNA-21 inhibitor)/RNATrans Mate complex was added to the petri dish (containing 400 μL DMEM) and incubated with HeLa cell for 24 h at 37 °C to obtain the transfected HeLa cells.

Apoptosis analysis by flow cytometry

MCF-7 cells were seeded into petri dishes and incubated for 48 h, and then AuNRs, AuNRs-DNA, AuNRs-DNA/FA, and AuNRs-DNA/FA: DOX nanocomposites were added to different petri dishes. In addition, the other two dishes were treated with PBS and complex respectively and irradiated with 808 nm pulse laser for 5 min (1000 mW). After incubation for 2 h, 100 μL trypsin was added to the petri dish respectively to harvest the cells. Then the cells were washed with cold PBS, and finally the dispersed cells were put into the 2-mL centrifuge tube. The collected cells were centrifuged at 559 g for 2 min, and 5 μL AnnxinV-FITC and 5 μL 7-AAD were added to the cells. After incubation for 10 min, the cells were centrifuged at 559*g* for 2 min. Finally, the cells were re-dispersed in the 0.5-mL centrifuge tube, and the apoptosis rate was detected by flow cytometry.

Results and discussion

Characterization of AuNRs and nanocomposites

AuNRs were prepared by the seed-mediated growth method and were characterized by TEM image. It can be seen from Fig. 1A that the nanomaterial showed regular rod-like structure and was dispersed in aqueous solution with CTAB as a protective agent. TEM image of Fig. 1A and **Fig. S1A** showed that the aspect ratios of AuNRs are 3:17 and 3:10, respectively. In addition, the absorption spectra of different nanoprobes were determined by UV-vis spectrometer, revealing a strong absorption in NIR region around 800 nm arising from AuNRs. After DNA was connected to the surface of AuNRs, a new absorption peak arose at 260 nm, which further proved that double-stranded DNA has been successfully modified to the surface of AuNRs. In order to realize the specific recognition ability of nanoprobe to MCF-7 cells, FA was modified to the surface of AuNRs-DNA, which could be confirmed by a new absorption peak at 380 nm. After that, DOX was inserted into the double-stranded DNA, and the related absorption peak of DOX was observed at 480 nm, as shown in Fig. 1B.

Moreover, the surface charge of AuNRs, AuNRs-DNA, AuNRs-DNA/FA, and AuNRs-DNA/FA: DOX was determined by zeta potential analysis, as shown in **Fig. S1B**. At the beginning, AuNRs carried an amount of positive electricity because of the protection by CTAB, and the zeta potential of surface became negative after being modified by DNA. Then, AuNRs-DNA was connected with FA, and the zeta potential increased gradually from −22.6 to −26.7 mV because of the introduction of negative-charged FA. Finally, DOX was inserted into double-stranded DNA, and the nanoprobe has been successfully prepared, and the zeta potential turned positive. The surface of cell membrane

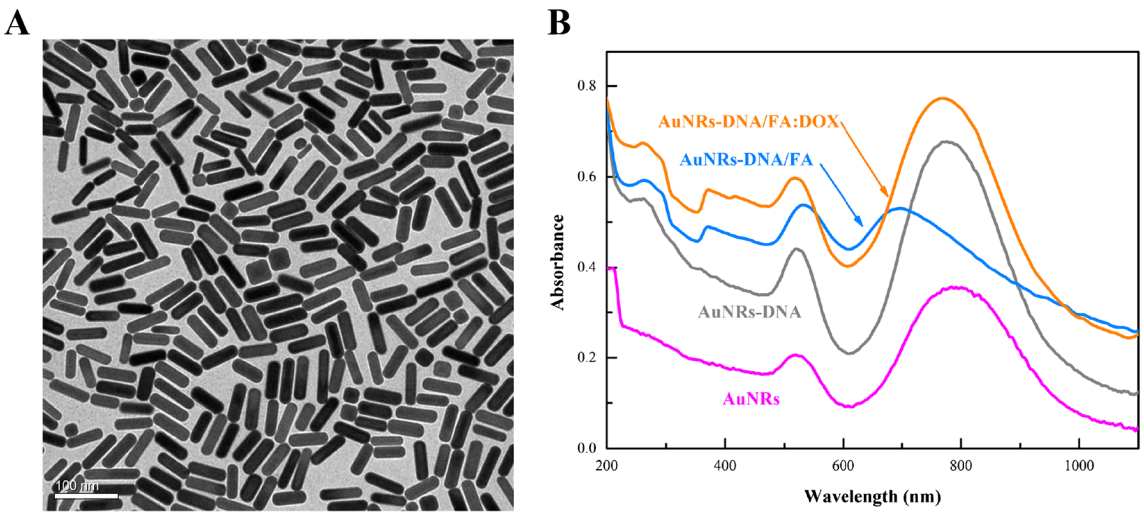

Fig. 1 **A** TEM image of AuNRs (The scale bar is 100 μm). **B** UV-vis absorption spectra of AuNRs, AuNRs-DNA, AuNRs-DNA/FA, and functionalized AuNRs-DNA/FA: DOX nanoprobe

is known to carry an amount of negative electricity, which can promote the uptake of nanoprobe by MCF-7 cells.

Optimization of pH conditions in vivo and in vitro

In order to improve the sensitivity of the nanocomposite for the detection of microRNA-21, the pH condition of the reaction was optimized. As shown in **Fig. S4**, the fluorescence signal of the nanoprobe interacting with the microRNA-21 in different pH conditions in vitro was explored, including pH value of 6, 6.5, 7, 7.3, 7.4, 7.5, 8, and 8.5. As shown in **Fig. S4**, the fluorescence signal reached the maximum in PBS of pH 7.4, whereas a higher or lower pH yielded the decreased fluorescence value due to RNA decomposition. In addition, the pH condition of the nanocomposite for the detection of microRNA-21 in vivo was optimized by confocal microscopy images, as shown in **Fig. S5**, and the maximum red fluorescence signal was obtained in PBS with a pH value of 7.4.

Detection of microRNA-21 in vitro

The prepared AuNRs-DNA/FA: DOX nanocomposite reacted with microRNA-21 and the fluorescence spectra of free DOX were measured for the purpose of verifying the feasibility of the experimental scheme. As shown in Fig. 2A, the free DOX showed a strong emission (red curve). After the connection of AuNRs with DOX, the fluorescence of DOX was quenched effectively by AuNRs due to Förster resonance energy transfer (FRET, black curve). The binding strength of the double-stranded DNA was weak, because there were three bases mismatched. When the nanoprobe was incubated with microRNA-21, it will compete with the double-stranded DNA, leading to

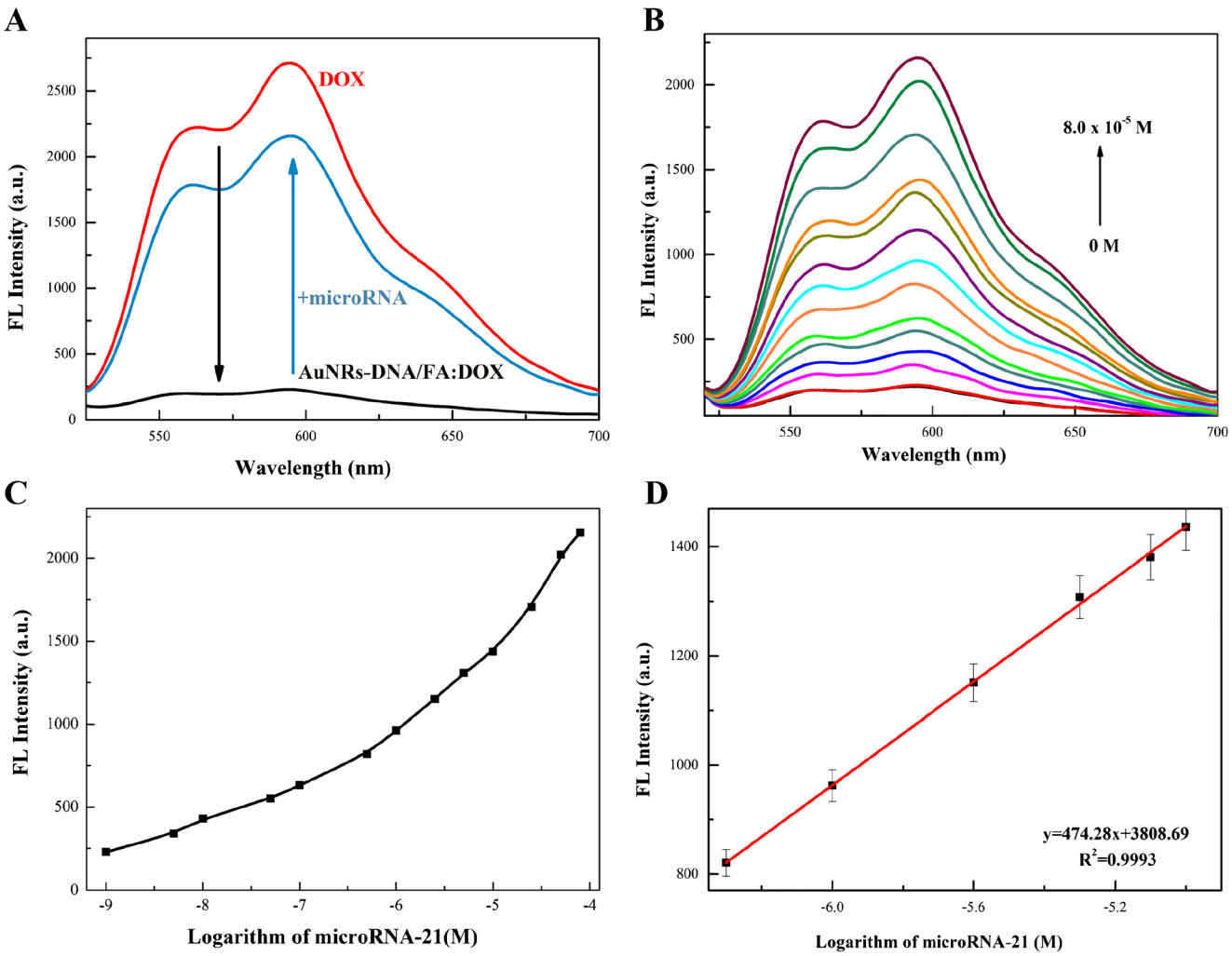

Fig. 2 **A** Fluorescence spectra of DOX (red curve) and AuNRs-DNA/FA: DOX in the presence (blue curve) or absence (black curve) of microRNA-21. **B** Fluorescence spectra of DOX with different concentrations of microRNA-21 (8.0×10^{-5}, 5.0×10^{-5}, 2.5×10^{-5}, 1.0×10^{-5}, 8.0×10^{-6}, 5.0×10^{-6}, 2.5×10^{-6}, 1.0×10^{-6}, 5.0×10^{-7}, 1.0×10^{-7}, 5.0×10^{-8}, 1×10^{-8}, 5×10^{-9}, 1.0×10^{-9} M). **C** The relationship curve of the fluorescence intensity at 595 nm versus the concentrations of microRNA-21. **D** Fitting logarithmic curve of the relative fluorescence intensity and the target microRNA-21 concentrations (1.0×10^{-5}, 8.0×10^{-6}, 5.0×10^{-6}, 2.5×10^{-6}, 1.0×10^{-6}, 5.0×10^{-7} M)

the release of DOX from the double-stranded DNA and the recovery of its fluorescence (blue curve). The fluorescence signal of DOX was measured after the nanocomposite probes were incubated with different concentrations of microRNA-21 at 37 °C, as shown in Fig. 2B and C. DOX exhibited red emission with a maximum fluorescence at 595 nm. With the increase of microRNA-21 concentration, the fluorescence intensity of DOX enhanced gradually. Additionally, there was a good linearity within microRNA-21 concentration range of 1.0×10^{-5} to 5.0×10^{-7} M ($R^2 = 0.9993$), offering a limit of detection as low as 2.11 nM according to the 3σ/k (where σ is the standard deviation of the blank and k is the slope of the calibration plot), as shown in Fig. 2D.

In the previous reports for microRNA-21 detection methods, the materials showed limited biocompatibility and stability. Moreover, the application scope of the detection can only be confined to the solution due to the limitations of the materials, besides the low level of microRNA-21 expression in living cells. Therefore, it is still a challenge to achieve the goal of rapid and sensitive detection for microRNA-21 in living cells. In this work, AuNRs were used as the carrier, and the modified PEG on the surface was to enhance the biocompatibility. FA was used as the receptor to achieve the targeted detection for microRNA-21 in MCF-7 cells. Moreover, compared with traditional biosensors, this method showed higher specificity. It can not only distinguish single base mismatch, but also has higher selectivity for other organic compounds in serum (**Table S1**) [29–33]. In addition, AuNRs showed a strong absorption in near-infrared (NIR) region due to the excitation of surface plasmon resonance (SPR) as descripted in Fig. 1B, so it can be used as a photothermal agent for cancer imaging and treatment.

Selectivity of AuNRs-DNA/FA: DOX nanocomposite

For practical biosensors, specificity is very important to prevent false positive or false negative signals. As shown in **Fig. S2A**, in order to distinguish the miRNAs with single base mutation, the prepared nanocomposites were reacted with ST1 (1 mismatch base), ST2 (two mismatch bases), and ST3 (three mismatch bases). The results showed that when the fluorescence signal of target microRNA-21 was defined as 100%, the relative fluorescence intensity of ST2 (two mismatched bases) and ST3 (three mismatched bases) was less than 11%. Even if there was only one single base mismatch, the relative fluorescence intensity of ST1 was below 24%. As shown in **Fig. S2B**, the nanocomposites showed good fluorescence response to target microRNA-21, and other RNA or interference compound in serum triggered little response. It is further confirmed that the probe has excellent selectivity, which provides a reliable guarantee for cell imaging.

Cytotoxicity assay of nano-drug carrier and nanocomposites

To evaluate the cytotoxicity of AuNRs-DNA/FA nanoparticles for MCF-7 cells and AuNRs-DNA/FA: DOX nanocomposites for normal cells (HEK 293 T cells), the survival rate was determined by CCK-8 in this study. As shown in **Fig. S3**, after incubation with 5 uL AuNRs-DNA/FA and AuNRs-DNA/FA: DOX for 0 h, 2 h, 4 h, 6 h, 8 h, 10 h, 12 h, 24 h, and 48 h respectively, MCF-7 and HEK 293 T cells were stained with CCK-8, respectively. After detection by enzyme labeling instrument, the cell survival rate was calculated by $(A_{test} / A_{control}) \times 100\%$. Learning from **Fig. S3**, the apoptosis rate rose slightly with the increase of incubation time, and the cell survival rate remained above 90% and 80% respectively after being incubated for 48 h. This result indicated that the nano-carrier exhibited good biocompatibility and low cytotoxicity, and AuNRs-DNA/FA: DOX composites have low damage to normal cells due to the unique targeting.

Imaging and detection of microRNA-21 in living cells

In this study, MCF-7 cells with a high microRNA-21 expression level were utilized as the cell model, and HeLa cells with a low microRNA-21 expression level were chosen as control. AuNRs-DNA/FA: DOX nanoprobes were incubated with MCF-7 cells and HeLa cells respectively at 37 °C for 2 h. The fluorescence imaging of cancer cells was observed by laser confocal microscope. As shown in Fig. 3, nanoprobe can specifically recognize MCF-7 cells because the surface of AuNRs-DNA/FA: DOX nanoprobe was modified with FA. Therefore, the uptake ability of MCF-7 cells for nanoprobe was much higher than that of HeLa cells, leading to a stronger fluorescent response in MCF-7 cells than that in HeLa cells.

In order to explore the drug release behavior of the nanoprobe in vivo, the AuNRs-DNA/FA: DOX nanoprobe was incubated with MCF-7 cells, and laser confocal microscope imaging was applied to track the fluorescence response. When the nanoprobe entered the cancer cell by endocytosis, microRNA-21 could compete with the double-stranded DNA with the release of red fluorescence signal. With the increase of incubation time, more nanocomposites were absorbed by cells with untied double-stranded DNA, leading to the gradual increase in the amount of drug release and the stronger red fluorescence signal, as shown in Fig. 4. In addition, under the irradiation of 808 nm NIR pulse laser (1000 mW), AuNRs could exert its intrinsic photothermal properties, which could accelerate the accumulation of drugs in the nucleus and further promote cell apoptosis.

MicroRNA-21 inhibitor is a single stranded RNA molecule, and its sequence can be complementary to the base sequence of

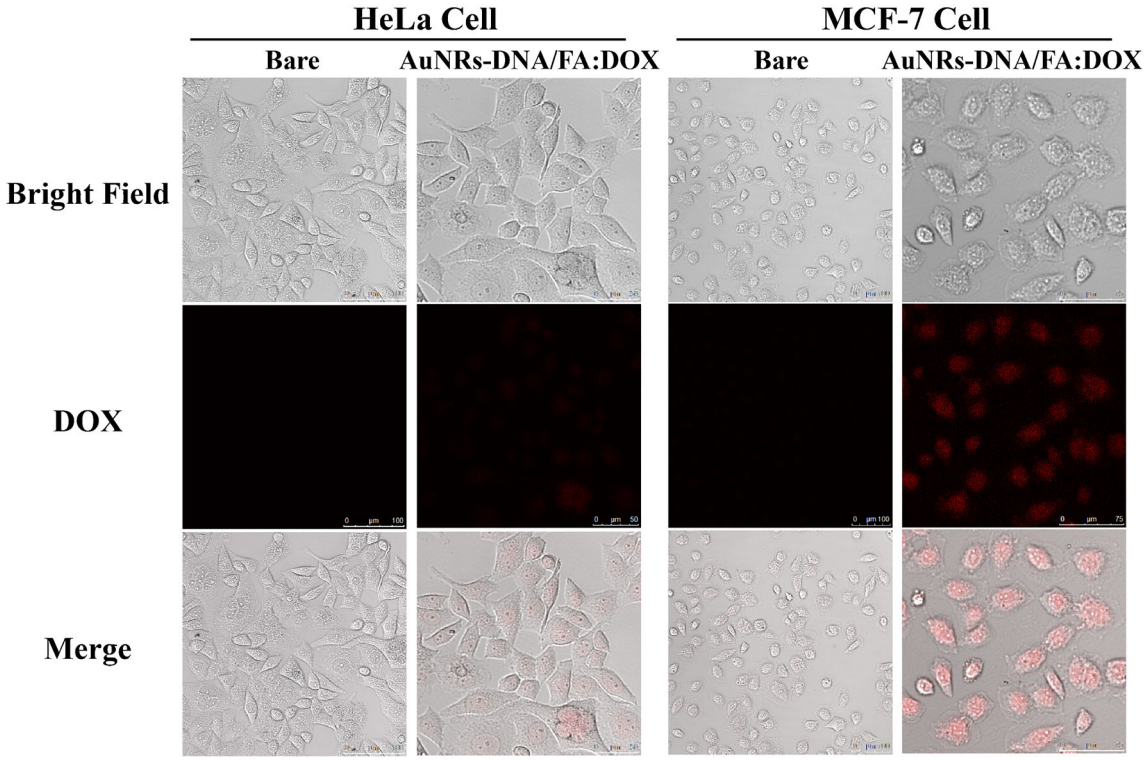

Fig. 3 Confocal microscopy images of MCF-7 cells and Hela cells after incubation with AuNRs-DNA/FA: DOX nanoprobes for 2 h

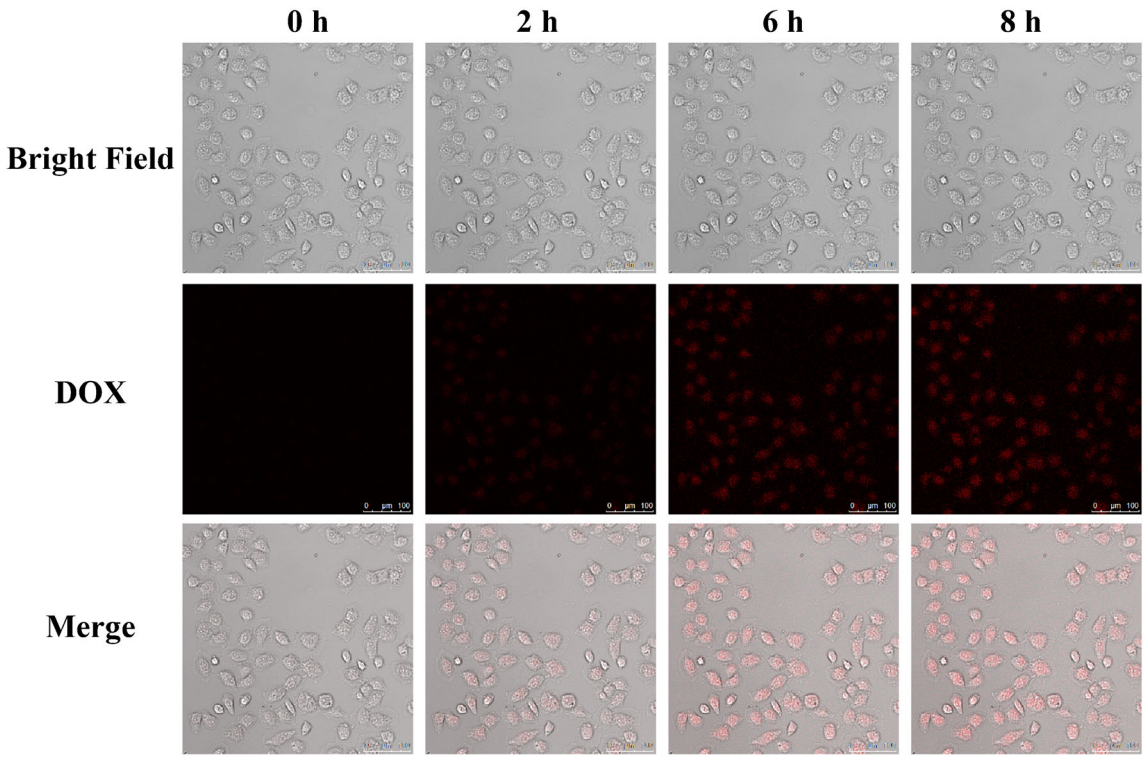

Fig. 4 Time-dependent fluorescence images of MCF-7 cells after incubation with AuNRs-DNA/FA: DOX nanocomposites for 0.0, 2.0, 6.0, and 8.0 h, respectively, and irradiation with 808 nm pulse laser for 5 min (1000 mW)

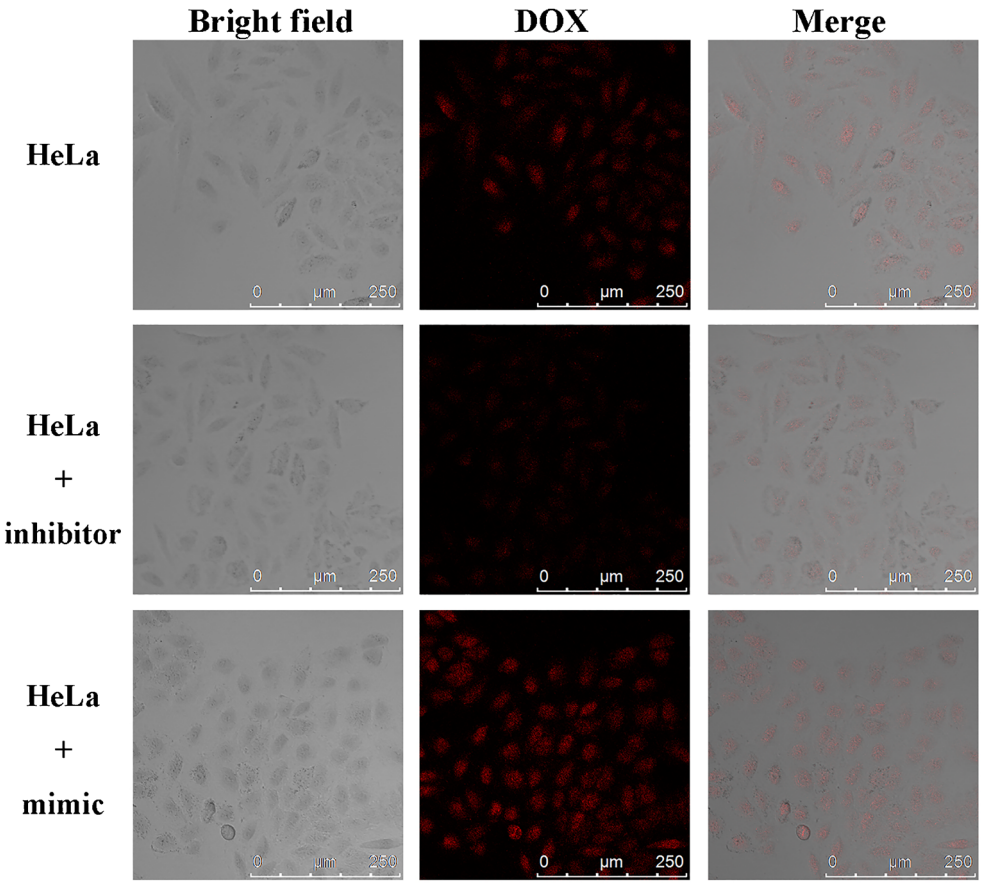

Fig. 5 Confocal microscopy images of HeLa cell incubated with nanocomposites for 2 h after pretreatment with microRNA-21 mimic and microRNA-21 inhibitor, respectively

miRNA-21 in HeLa cells and reduce the concentration of microRNA-21 in cells. On the contrary, microRNA-21 mimic has the opposite effect, which can increase the concentration of microRNA-21 in cells. As shown in Fig. 5, compared with the untreated cells, the fluorescence signal of the cells treated with microRNA-21 inhibitor was significantly decreased. On the contrary, the fluorescence signal of the cells treated with microRNA-21 mimics was significantly enhanced.

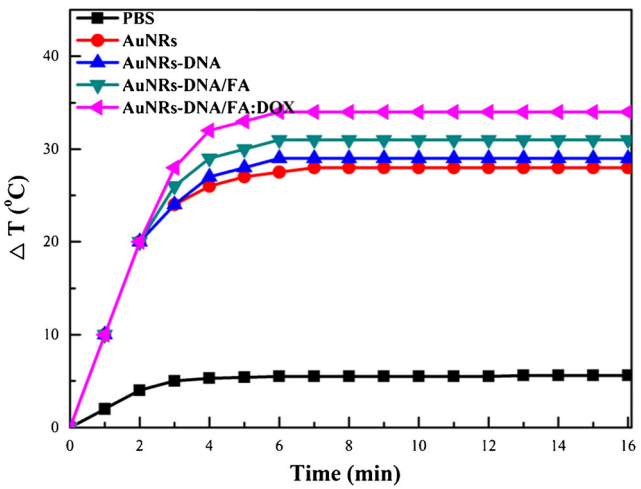

Fig. 6 The photothermal effects of PBS, AuNRs, AuNRs-DNA, AuNRs-DNA/FA, and AuNRs-DNA/FA: DOX with 808 nm pulse laser for 5 min (1000 mW)

Photothermal effects of different nanocomposites

To evaluate the photothermal effects of different nanocomposites, PBS, AuNRs, AuNRs-DNA, AuNRs-DNA/FA, and AuNRs-DNA/FA: DOX complex were irradiated by 808 nm NIR laser, as shown in **Fig. S3**. The temperature of PBS was hardly raised after being irradiated by laser lamp. However, the temperature of AuNRs and its complex gradually went up under the irradiation of laser lamp, which reached the maximum within 8 min. It can be seen from Fig. 6 that the temperature of AuNRs and AuNRs DNA can reach 45 °C after being irradiated with 808 nm pulse laser for 5 min, while the temperature of AuNRs DNA/FA and AuNRs DNA/FA: DOX can reach 52 °C after being irradiated. The main reasons for the difference of photothermal effects of different composites are as follows. On the one hand, the irradiated area by pulse laser was uneven, and the photothermal effect was relatively poor because of the lower dispersion and higher aggregation of AuNRs or AuNRs-DNA. On the other hand, part of the AuNRs can be dissolved at high temperature under irradiation of laser, resulting in the decrease of photothermal effect. The

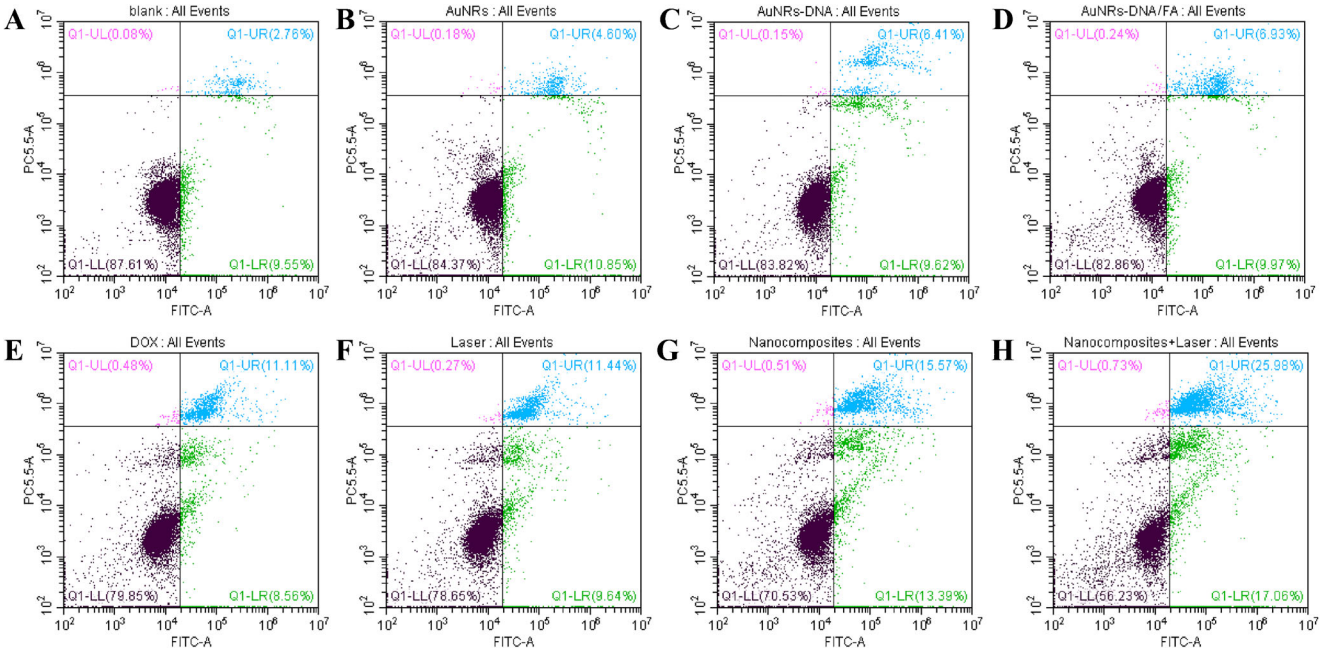

Fig. 7 Analysis of cell apoptosis for MCF-7 cells upon treatment with PBS solution (**A**), AuNRs (**B**), AuNRs-DNA (**C**), AuNRs-DNA/FA (**D**), DOX (**E**), 808 nm pulse laser for 5 min (1000 mW) (**F**), AuNRs-DNA/FA: DOX (**G**), and AuNRs-DNA/FA: DOX irradiated with 808 nm pulse laser for 5 min (1000 mW) (**H**)

introduction of PEG with good biocompatibility can increase the dispersion of AuNRs DNA/FA and AuNRs DNA/FA: DOX, and the modification of PEG can effectively protect AuNRs from the thermal decomposition, thus significantly improving the photothermal effect. This high-efficiency heating method can promote the permeability of the drug in tumor tissue and blood circulation, achieving an improved therapeutic effect ultimately.

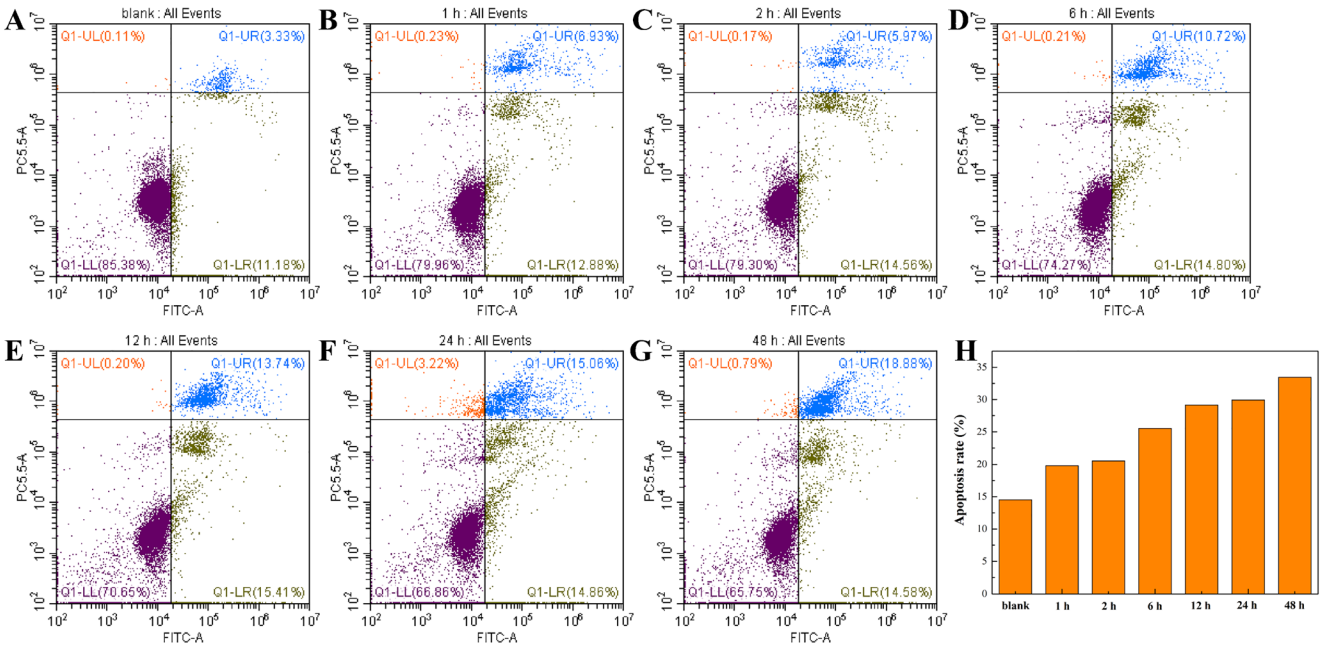

Fig. 8 Analysis of cell apoptosis for MCF-7 cells upon treatment with PBS (**A**), AuNRs-DNA/FA: DOX nanoprobe for 1 (**B**), 2 (**C**), 6 (**D**), 12 (**E**), 24 (**F**), and 48 h (**G**), respectively. The apoptosis distribution histogram of MCF-7 cells treated with AuNRs-DNA/FA: DOX nanoprobe for different time (**H**)

Apoptosis assay of different nanocomposites

Furthermore, the proapoptosis capability of nanocomposites was explored. After incubation with AuNRs, AuNRs-DNA, AuNRs-DNA/FA, free DOX, and AuNRs-DNA/FA: DOX complex, respectively, MCF-7 cells were stained with apoptosis kit and analyzed by flow cytometry, as shown in Fig. 7. The cells treated by PBS were taken as control. The apoptosis ratio of AuNRs, AuNRs-DNA, and AuNRs-DNA/FA was determined to be 15.45%, 16.03%, and 16.90%, respectively. Compared with the blank group, the nano-drug carrier exhibited lower cytotoxicity and favorable biocompatibility. The apoptosis rates of free DOX and AuNRs-DNA/FA: DOX nanoprobes were found to be 19.67% and 28.96%, respectively, and AuNRs-DNA/FA: DOX nanocomposite showed a better proapoptosis capability, which provided a reliable scheme for biologically clinical diagnosis and treatment. In addition, as shown in Fig. 7F, the AuNRs could exert its photothermal effect after the cells were treated with AuNRs and irradiated by 808 nm pulse laser for 5 min (1000 mW), with apoptosis ratio determined to be 21.08%. After the incubation with nanocomposites and irradiation with 808 nm pulse laser for 5 min (1000 mW), the cell apoptosis ratio was found to be 43.04% as shown in Fig. 7H, achieving the purpose of combining photothermal therapy with chemotherapy.

It has been confirmed that the AuNRs-DNA/FA: DOX nanocomposite has a good therapeutic effect on MCF-7 cells by the aforementioned experimental results. Thus, to evaluate the apoptosis feasibility of the well-designed probe, MCF-7 cells were cultured with AuNRs-DNA/FA: DOX for 1, 2, 6, 12, 24, and 48 h, respectively, and analyzed by Annex in V-FITC/7-AAD double staining assay. As shown in Fig. 8, the apoptosis rate was 19.81% after 1 h culture, and the apoptosis rate rose significantly with the increase of incubation time. When the nanoprobe was incubated with cancer cells for 48 h, the apoptosis rate of necrotic and late apoptotic areas gradually increased, and the apoptosis rate could reach 33.46%. Meanwhile, there was a gradual enhancement of the FITC-A fluorescence in MCF-7 cells upon incubation time (**Fig. S6**).

From the above results, it is not difficult to see that the designed nanocomposites showed effective detection and therapeutic performance, but there are still some shortcomings. First, the accurate determination of intracellular microRNA-21 was not achieved. In the follow-up study, we can introduce high quantum yield fluorophores to build a ratiometric detection mode to achieve quantitative analysis in cells. Second, the photothermal properties of gold nanorods are limited, so it is possible to design better photothermal materials instead of AuNRs.

Conclusions

In this work, AuNRs-DNA/FA: DOX nanoprobe functionalized with microRNA-21-induced drug release capability was designed as a biosensor platform for tumor-targeted therapy. The specific recognition ability of FA can promote MCF-7 cells endocytosis of nano-drug carriers, and DOX can be effectively released from double-stranded DNA. Hence, the cooperative diagnosis and treatment of MCF-7 cells can be realized by photothermotherapy and chemotherapy. This nanoprobe put forward a feasible strategy for microRNA-21 determination and target drug delivery with facile preparation and good biocompatibility, which is of significant importance in the field of anti-tumor therapy and the diagnosis of human disease.

Supplementary Information The online version contains supplementary material available at https://doi.org/10.1007/s00604-021-04917-8.

Acknowledgements We gratefully acknowledge financial support from the National Natural Science Foundation of China (21904077, 22074074, 22004078).

Declarations

Conflict of interest The authors declare no competing interests.

References

1. Ambros V (2004) The functions of animal microRNAs. Nature 431(7006):350–355
2. Cissell K A, Shrestha S, Deo S K (2007) MicroRNA detection: Challenges for the analytical chemist. Anal Chem 79 (13), 4754–61
3. Dong H, Lei J, Ding L, Wen Y, Ju H, Zhang X (2013) MicroRNA: function, detection, and bioanalysis. Chem Rev 113(8):6207–6233
4. Ma J, Dong C, Ji C (2010) MicroRNA and drug resistance. Cancer Gene Ther 17(8):523–531
5. Kutanzi KR, Yurchenko OV, Beland FA, Checkhun VF, Pogribny IP (2011) MicroRNA-mediated drug resistance in breast cancer. Clin Epigenetics 2(2):171–185
6. Ji X, Wang Z, Niu S, Ding C (2020) DNAzyme-functionalized porous carbon nanospheres serve as a fluorescent nanoprobe for imaging detection of microRNA-21 and zinc ion in living cells. Mikrochim Acta 187(4):249
7. Xu W, Zhao A, Zuo F, Khan R, Hussain HMJ, Chang J (2020) Au@Ag core-shell nanoparticles for microRNA-21 determination based on duplex-specific nuclease signal amplification and surface-enhanced Raman scattering. Mikrochim Acta 187(7):384
8. Zhang P, He Z, Wang C, Chen J, Zhao J, Zhu X, Li CZ, Min Q, Zhu JJ (2015) In situ amplification of intracellular microRNA with MNAzyme nanodevices for multiplexed imaging, logic operation, and controlled drug release. ACS Nano 9(1):789–798

9. Chen N, Li J, Feng X, Yang Y, Zhu L, Chen X, Liu X, Li Y, Wang C, Xia L (2020) Label-free and self-assembled fluorescent DNA nanopompom for determination of miRNA-21. Mikrochim Acta 187(8):432
10. Varallyay E, Burgyan J, Havelda Z (2008) MicroRNA detection by northern blotting using locked nucleic acid probes. Nat Protoc 3(2): 190–196
11. Kim SW, Li Z, Moore PS, Monaghan AP, Chang Y, Nichols M, John B (2010) A sensitive non-radioactive northern blot method to detect small RNAs. Nucleic Acids Res 38(7):e98
12. Liu CG, Calin GA, Volinia S, Croce CM (2008) MicroRNA expression profiling using microarrays. Nat Protoc 3(4):563–578
13. Tian T, Wang J, Zhou X (2015) A review: microRNA detection methods. Org Biomol Chem 13(8):2226–2238
14. Nelson PT, Baldwin DA, Scearce LM, Oberholtzer JC, Tobias JW, Mourelatos Z (2004) Microarray-based, high-throughput gene expression profiling of microRNAs. Nat Methods 1(2):155–161
15. Gewirtz DA (1991) Does bulk damage to DNA explain the cytostatic and cytotoxic effects of topoisomerase II inhibitors? Biochem Pharmacol 42(12):2253–2258
16. Wang F, Wang YC, Dou S, Xiong MH, Sun TM, Wang J (2011) Doxorubicin-tethered responsive gold nanoparticles facilitate intracellular drug delivery for overcoming multidrug resistance in cancer cells. ACS Nano 5(5):3679–3692
17. Wei Y, Chen Q, Wu B, Zhou A, Xing D (2012) High-sensitivity in vivo imaging for tumors using a spectral up-conversion nanoparticle $NaYF_4$: Yb^{3+}, Er^{3+} in cooperation with a microtubulin inhibitor. Nanoscale 4(13):3901–3909
18. Liu J, Zhang L, Lei J, Ju H (2015) MicroRNA-responsive cancer cell imaging and therapy with functionalized gold nanoprobe. ACS Appl Mater Interfaces 7(34):19016–19023
19. Grabinski C, Schaeublin N, Wijaya A, D'Couto H, Baxamusa SH, Hamad-Schifferli K, Hussain SM (2011) Effect of gold nanorod surface chemistry on cellular response. ACS Nano 5(4):2870–2879
20. Zijlstra P, Paulo PM, Orrit M (2012) Optical detection of single non-absorbing molecules using the surface plasmon resonance of a gold nanorod. Nat Nanotechnol 7(6):379–382
21. Kong G, Braun R, Dewhirst M (2000) Hyperthermia enables tumor-specific nanoparticle delivery: effect of particle size. Cancer Res 60:4440–4445
22. Zhao P, Zheng M, Yue C, Luo Z, Gong P, Gao G, Sheng Z, Zheng C, Cai L (2014) Improving drug accumulation and photothermal efficacy in tumor depending on size of ICG loaded lipid-polymer nanoparticles. Biomaterials 35(23):6037–6046
23. Kong G, Dewhirst MW (1999) Review hyperthermia and liposomes. Int J Hyperth 15(5):345–370
24. Karino T, Koga S, Maeta M (1988) Experimental studies of the effects of local hyperthermia on blood flow, oxygen pressure and pH in tumors. Jpn J Surg 18(3):276–283
25. Wang H, Zhao R, Li Y, Liu H, Li F, Zhao Y, Nie G (2016) Aspect ratios of gold nanoshell capsules mediated melanoma ablation by synergistic photothermal therapy and chemotherapy. Nanomedicine 12(2):439–448
26. Cheng L, Liu J, Gu X, Gong H, Shi X, Liu T, Wang C, Wang X, Liu G, Xing H, Bu W, Sun B, Liu Z (2014) PEGylated WS(2) nanosheets as a multifunctional theranostic agent for in vivo dual-modal CT/photoacoustic imaging guided photothermal therapy. Adv Mater 26(12):1886–1893
27. Song XR, Wang X, Yu SX, Cao J, Li SH, Li J, Liu G, Yang HH, Chen X (2015) Co(9) Se(8) nanoplates as a new theranostic platform for photoacoustic/magnetic resonance dual-modal-imaging-guided chemo-photothermal combination therapy. Adv Mater 27(21):3285–3291
28. Wen L, Chen L, Zheng S, Zeng J, Duan G, Wang Y, Wang G, Chai Z, Li Z, Gao M (2016) Ultrasmall biocompatible WO_3^- x nanodots for multi-modality imaging and combined therapy of cancers. Adv Mater 28(25):5072–5079
29. Zhou Y, Zhang Z, Xu Z, Yin H, Ai S (2012) MicroRNA-21 detection based on molecular switching by amperometry. New J Chem 36(10):1985–1991
30. Azzouzi S, Fredj Z, Turner APF, Ali MB, Mak WC (2019) Generic neutravidin biosensor for simultaneous multiplex detection of microRNAs via electrochemically encoded responsive nanolabels. ACS Sens 4(2):326–334
31. Zhao H, Qu Y, Yuan F, Quan X (2016) A visible and label-free colorimetric sensor for miRNA-21 detection based on peroxidase-like activity of graphene/gold-nanoparticle hybrids. Anal Methods 8:2005–2012
32. Zuo C, Guo Y, Li J, Peng Z, Bai S, Yang S, Wang D, Chen H, Xie G (2021) A nanoprobe for fluorescent monitoring of microRNA and targeted delivery of drugs. RSC Adv 11:8871–8878
33. Wang A, Yang X, Wang K, Huang J (2021) Orderly assembled, self-powered FRET flares for microRNA imaging in live cells. Anal Chem 93(15):6270–6277